

# Folding style controlled by intermediate decollement thickness change in the Lurestan region (NW of the Zagros fold-and-thrust belt), using analogue models

Ali Farzipour Saein<sup>1</sup>

Received: 16 April 2016 / Accepted: 25 June 2016 / Published online: 9 July 2016  
© Springer-Verlag Berlin Heidelberg 2016

**Abstract** The basal and intermediate decollements play an important role in structural style of fold-and-thrust belts. The decollement units, or different mechanical stratigraphy within the rock units, are not uniform throughout the ZFTB and show a strong spatial variation. The Lurestan region with varied thickness of the intermediate decollement in its northern and southern parts is one of the most important parts of the Zagros fold-and-thrust belt, regarding its hydrocarbon exploration–extraction projects. Thickness variation of the intermediate decollement in different parts of the Lurestan region allows us to address its role on folding style. Based on scaled analogue modeling, this study outlines the impact of thickness and facies variation of sedimentary rocks in the northern and southern parts of this region on folding style. Two models simulated the mechanical stratigraphy and its consequent different folding styles of the northern and southern parts of the region. In the models, only thickness of the intermediate decollement (thick and thin) for the northern and southern parts of the Lurestan region was varied. Detached minor folds above the intermediate decollement were created in response to the presence of the thicker intermediate decollement, northern part of the study area, which consequently deformed complexly and disharmonically folded, in contrast to polyharmonic folding style in the section, compared to polyharmonic folding style in the southern part, where thin intermediate decollement exists. The model results documented that thickness variation of intermediate decollement levels could explain complex and different folding styles in

natural examples which must be taken into account for hydrocarbon exploration throughout these areas.

**Keywords** Zagros fold-and-thrust belt · Intermediate decollement · Analogue modeling · The Lurestan region

## Introduction

Recent regional studies have shown that mechanical stratigraphy (Mukherjee and Biswas 2015; Mukherjee and Mulchrone 2015; Mulchrone and Mukherjee 2015) has an essential role in governing the fold style in the Zagros (Blanc et al. 2003; Homke et al. 2004; Koyi et al. 2004; Sherkati and Letouzey 2004; Molinaro et al. 2005; Sephehr et al. 2006; Sherkati et al. 2006; Farzipour Saein et al. 2009). There are many fold-and-thrust belts where the basal and intermediate decollements play an important role in their structural style, e.g., Zagros (Koyi et al. 2004; Farzipour Saein et al. 2009), Po Basin (Massolli et al. 2006), Pyrennese (Koyi and Sans 2003). The effect of decollement has been studied by different workers using field observations and analytical, numerical and analogue modeling approaches (Chapple 1978; Davis and Engelder 1985; Butler et al. 1987; Cobbold et al. 1989; McClay 1989; Price and Cosgrove 1990; Buchanan and McClay 1991; Dixon and Liu 1992; Liu et al. 1992; Talbot 1992; Treloar et al. 1992; Weimer and Buffler 1992; Cobbold et al. 1995; Harrison and Pattern 1995; Letouzey et al. 1995; Sans and Vergés 1995; Blanc et al. 2003; Homke et al. 2004; Koyi et al. 2004; Sherkati and Letouzey 2004; Molinaro et al. 2005; Sephehr et al. 2006; Sherkati et al. 2006; Farzipour Saein et al. 2009; Vergés et al. 2011; Farzipour Saein and Koyi 2014). Several studies documented that detachment folding was affected by different

✉ Ali Farzipour Saein  
asaein@gmail.com

<sup>1</sup> Department of Geology, Faculty of Sciences, University of Isfahan, P. O. Code: 81746- 73441 Isfahan, Iran

decollement units in the Zagros fold-and-thrust belt, ZFTB (e.g., O'Brien 1950, 1957; Sherkati and Letouzey 2004; Farzipour Saein et al. 2009; Vergés et al. 2011; Farzipour Saein and Koyi 2014). The decollement units, or different mechanical stratigraphy within the rock units, are not uniform throughout the ZFTB and show a strong spatial variation (Koyi et al. 2004; Sherkati et al. 2006; Farzipour Saein et al. 2009; Farzipour Saein and Koyi 2014). The role of various decollement levels on structural style is well documented in many folded belts (e.g., Koyi 1988; Davis and Engelder 1985; Letouzey et al. 1995; Cotton and Koyi 2000; Bahroudi and Koyi 2003; Bahroudi and Koyi 2003; Nilforoushan et al. 2008; Farzipour Saein et al. 2009; Vergés et al. 2011). Using scaled analogue models, Farzipour Saein and Koyi (2014) documented the effect of lateral thickness variation of an intermediate decollement on the propagation of deformation front. However, thickness variation of the intermediate decollement in different parts of the Lurestan region (Farzipour Saein et al. 2009) allows us to address its role on folding style. The structural style of the folds from the central part of the Lurestan region has been studied by balanced cross sections, geological maps, seismic profiles, stratigraphic surface sections and well data which highlight difference in folding style across the area (Farzipour Saein et al. 2009). The vertical and lateral changes in folding style indicate mechanostratigraphy within the sedimentary units (Farzipour Saein et al. 2009; Vergés et al. 2011).

The main aim of this paper is to investigate folding style in the Lurestan region (Fig. 1) based on scaled analogue modeling, to outline the impact of thickness and facies variation of sedimentary rocks in the northern and southern parts of this region on folding style. This work uses results of scaled sandbox models shortened from one end to explain the variation in folding style between areas with thick versus thin intermediate decollement, sharing similar basal friction.

### The prototype

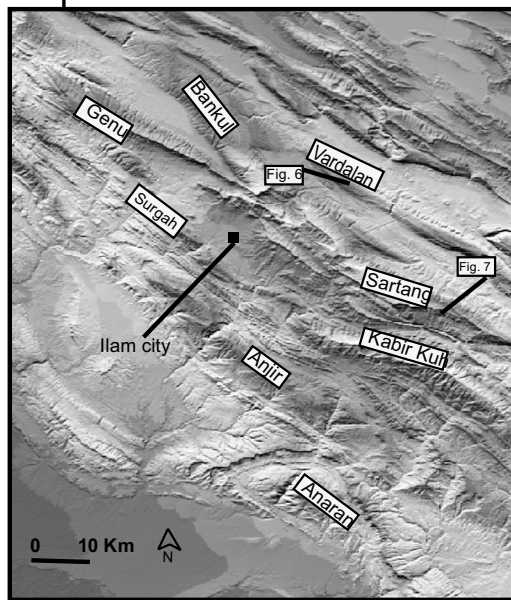
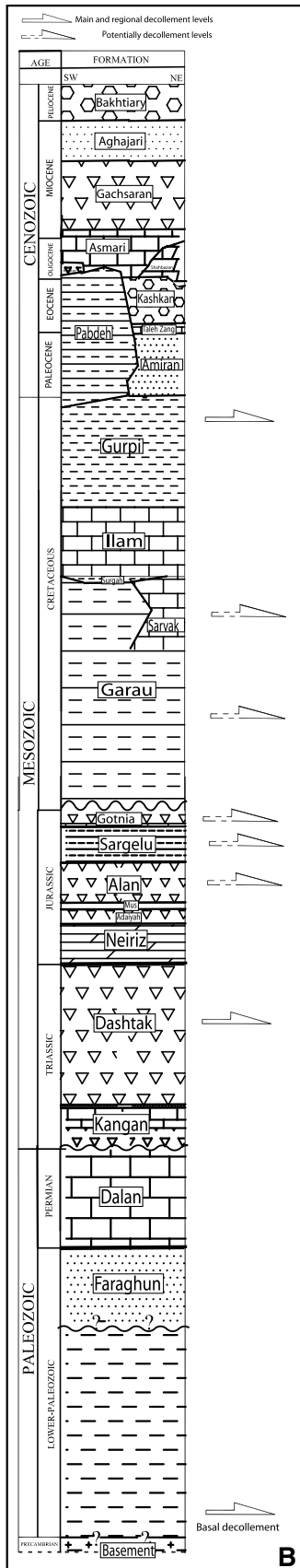
The Zagros basin was part of the stable supercontinent of Gondwana in Paleozoic time, a passive margin in the Mesozoic, and a convergent orogeny in the Cenozoic (Stocklin 1968; Berberian 1995; Bahroudi and Koyi 2004; Farzipour Saein et al. 2009; Casciello et al. 2009; Vergés et al. 2011; Farzipour Saein et al. 2013).

The ZFTB, as a part of the extensive Alpine–Himalayan orogeny system, can be divided into several zones, with different structural styles and sedimentary history, reflecting different deformation accommodated along the belt (Falcon 1969; Stocklin 1968; Falcon 1974; Haynes and McQuillan 1974; Berberian and King 1981; Motiee 1994; Berberian 1995; Bahroudi and Koyi 2004; Farzipour Saein et al.

**Fig. 1** **a** The *location map* of the Lurestan region (the study area) with the main structural features, subdivision of the Zagros fold-and-thrust belt and the location of the simplified structural cross sections throughout the Lurestan region. **b** The generalized mechanical stratigraphic column and potential decollement levels for the study area, based on stratigraphic surface sections, well data and field observation (modified after Farzipour Saein et al. 2009)

2009, 2013; Farzipour Saein and Koyi 2014; Fig. 1a). The simply folded zone as one of the important structural zones of the ZFTB can be divided, along strike from the east to the west, into the Fars, Izeh, Dezful embayment and Lurestan regions (McQuillan 1991; Berberian 1995; Farzipour Saein et al. 2009; Farzipour Saein and Koyi 2014; Fig. 1a). The Lurestan region in NW of the Zagros fold-and-thrust belt (ZFTB) has a long history of hydrocarbon exploration and production (Farzipour Saein et al. 2009). The eastern limit of the Lurestan region is separated from the Dezful embayment and the Izeh zone by the Balaroud Fault during Jurassic–Cretaceous (Hessami et al. 2001a, b; Blanc et al. 2003; Sepehr and Cosgrove 2004; Farzipour Saein et al. 2009; Casciello et al. 2009; Vergés et al. 2011; Farzipour Saein and Koyi 2014). To the NW, the Lurestan region is separated from the Kirkuk embayment by the Khanaqin Fault (Farzipour Saein et al. 2009, Fig. 1a). Structural style in different parts of the Lurestan, disharmonic folding style, during Oligocene to Tertiary (Berberian and King 1981; Ahmadhadi et al. 2007), in the south and polyharmonic in the north, are very well documented based on the field, seismic and well data (Farzipour Saein et al. 2009; Casciello et al. 2009).

In the Lurestan region, Early Paleozoic sediments rest directly on the highly metamorphosed Proterozoic Pan-African basement (Farzipour Saein et al. 2009; Letouzey et al. 1995). Sediments of the Lurestan salient are mostly pelagic carbonates, rich in organic materials, marine shale and evaporates (Fig. 1b). In this region, there are several formations that, based on their lithology and structural evidences (Farzipour Saein et al. 2009), have acted as decollement levels (e.g., Pabdeh, Gurpi, Surgah, Sarvak, Garau, Gotnia, Alan, Adaiyah, Dashtak and Lower Paleozoic sediments; see Fig. 1b for their lithology and age). The generalized stratigraphic framework through the Lurestan region showed that there are lateral facies changes within the main formations comparing the north part of the region to its southern part which consequently has caused different mechanical stratigraphy characteristics between the two parts (Farzipour Saein et al. 2009; Fig. 2a, b). Farzipour Saein et al. (2009) documented that thickness and facies changes of some formations that may have acted as intermediate decollement unit across the region cause lateral variation in folding pattern. From the north, where increased thickness of the intermediate decollement has led to decoupling at different structural levels, strongly



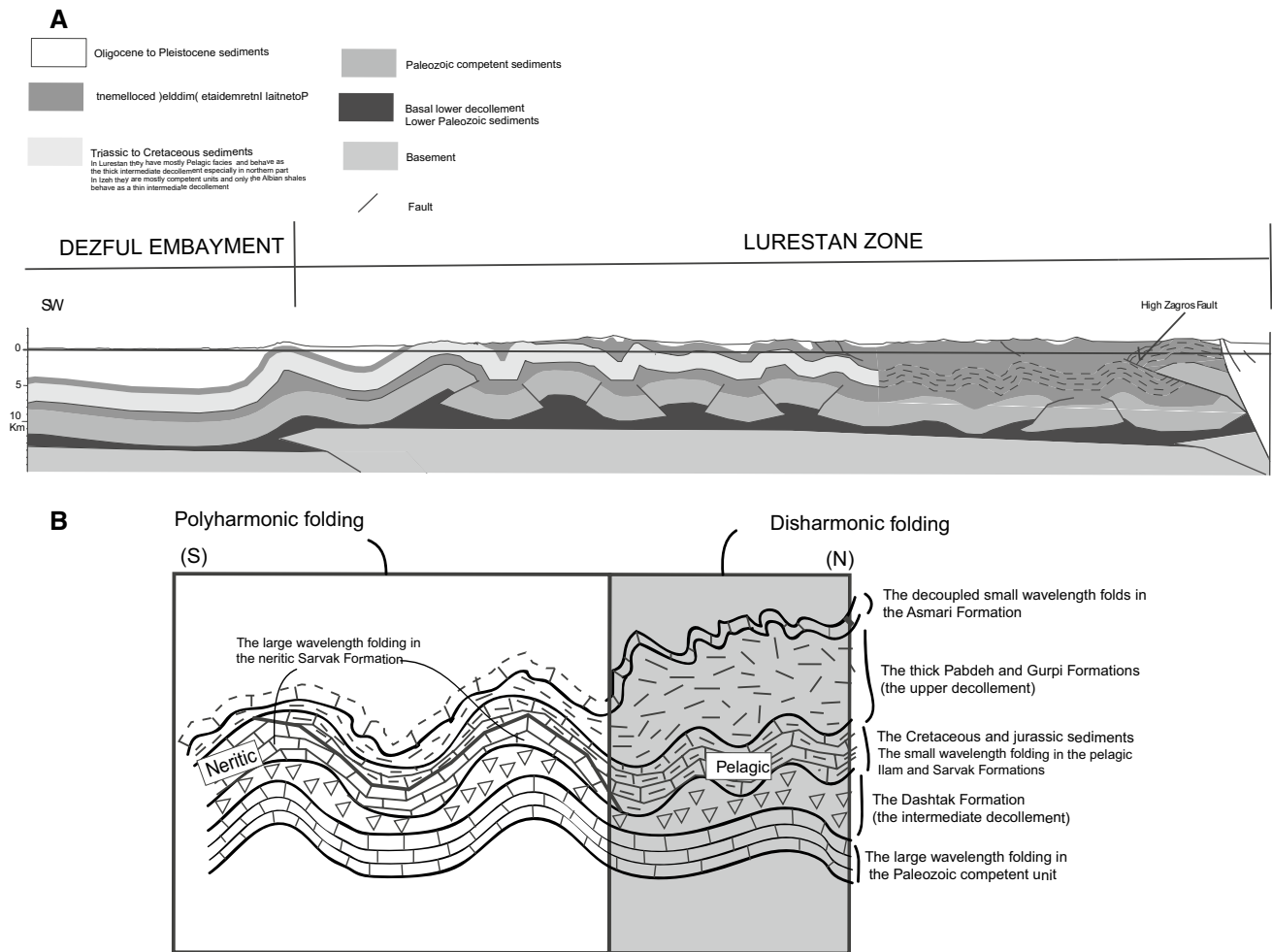


**Fig. 2** a Simplified structural cross sections in Lurestan region showing variable thickness of the intermediate decollement and different structural styles in the northern and southern parts of the region. See (Fig. 1a) for the location (modified after Farzipour Saein et al. 2009).

**b** A conceptual model explaining distribution of the folding patterns (disharmonic vs. polyharmonic) from north to south across the Lurestan region

disharmonic folding changes to polyharmonic folds in the south, where the different structural levels are not strongly coupled due to the thinner intermediate decollement unit (Fig. 2a, b). The folding styles of the discrete domains across the variable substrates resemble structural cross sections from the northern part (with thicker intermediate decollement) and southern part (with thinner intermediate decollement) of the Lurestan region (Fig. 2).

### Modeling strategy

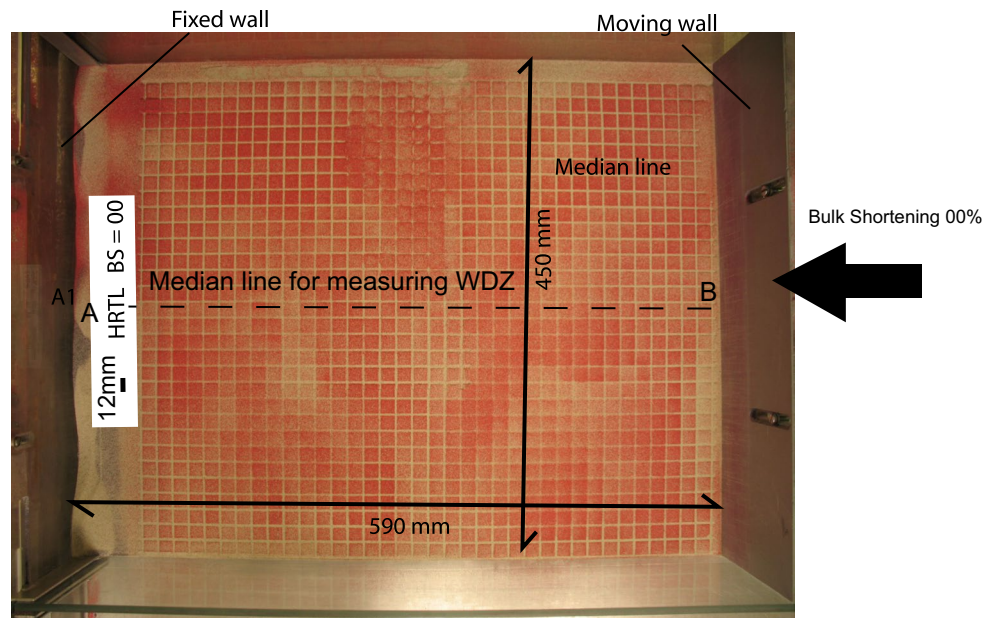
Different evidences indicate that there is a clear difference in the thicknesses of the intermediate decollement horizons between the northern and southern parts of the Lurestan (Farzipour Saein et al. 2009). On this basis, this study focuses on modeling of changes in thickness of the intermediate decollement (one model with thicker decollement

2 cm, simulating the northern part, and the other one with thinner, 0.5 cm, intermediate decollement simulating the southern part of the Lurestan region). Both models have similar configuration of basal decollement. Two models were run in order to simulate the mechanical stratigraphy and its consequent different folding styles of the northern and southern parts of the region. Both of these models were shortened from one end with the same speed simulating the shortening in the ZFTB. In the models, only thickness of the intermediate decollement (thick and thin) for the northern and southern parts of the Lurestan was varied (Fig. 3).

### Material and model setup

Dry loose sand, viscous silicon putty (polydimethylsiloxane, PDMS) and glass beads were used to simulate a

**Fig. 3** The models setup and also schematic sections through-out modeling materials for the models 1 and 2. The only difference between the two models is existence of the thicker (20 mm) intermediate decollement within model 1 comparing the thinner (5 mm) intermediate decollement for model 2



Model 1 (Northern part of the Lurestan)

	A	B	
4 mm	Loose sand		Competent unit
20 mm	Micro glass beads		Middle decollement
10 mm	Loose sand		Competent unit
10 mm	SGM 36 (viscus layer)		Basal decollement

Model 2 (Southern part of the Lurestan)

	A	B	
4 mm	Loose sand		Competent unit
5 mm	Micro glass beads		Middle decollement
10 mm	Loose sand		Competent unit
10 mm	SGM 36 (viscus layer)		Basal decollement

competent sedimentary layer, basal decollement and intermediate decollement, respectively, as has been the case in many previous models (Davy and Cobbold 1991; Weijermars et al. 1993; Cotton and Koyi 2000; Bonini 2001; Costa and Vendeville 2002; Bahroudi and Koyi 2003; Nilforoushan et al. 2008; Farzipour Saein and Koyi 2014). The bulk density of the sand (white and gray in color) used in the models was  $\rho = 1550 \text{ kgm}^{-3}$  with a cohesive strength  $C = 140 \text{ Pa}$ , coefficient of internal friction  $= 0.73$  and an average grain size of about  $\geq 35 \text{ }\mu\text{m}$  (Cotton and Koyi 2000). The Newtonian viscous material PDMS (manufactured by Dow Corning Ltd., Manchester, UK) has a density of  $\rho = 987 \text{ kg m}^{-3}$  and an effective viscosity of  $\eta = 5 \times 10^4 \text{ Pas}$  at room temperature at  $\sim 20 \text{ }^\circ\text{C}$  (Weijermars 1986). Indeed, glass microbeads have been regarded

as suitable materials for simulating weak layers (Massoli et al. 2006). This material consists of almost perfect spherical grains and has an angle of internal friction, consistently lower than the quartz sand. The glass microbeads, provided by CBC Ytfinish Ab, are almost perfect (simulating the incompetent intermediate rock units) spherical grains composed mainly of quartz glass (with minor components of sodium and calcium glass) with a grain size ranging between 100 and 105 microns and a bulk density of  $1.5 \text{ g cm}^{-3}$ . Their coefficient of friction is  $\mu = 0.37$  ( $\varphi = 20^\circ$ , Farzipour Saein and Koyi 2014). The layered sand simulated the competent sedimentary units in the Zagros fold-and-thrust belt, whereas the glass microbeads simulated the intermediate decollement, and PDMS simulated a viscous substrate (e.g., Hormoz Salt; Mukherjee

et al. 2010). Indeed, the base of each model was horizontally resting on a flat metal basal the crystalline basement.

Two rectangular models were prepared with glass walls, and initial dimensions of 590 × 450 mm placed horizontally on a metal sheet representing a rigid flat basement. A square grid acting as passive markers (12 × 12 mm each one) was imprinted on the surface of the models. Boundary effect was visible within a 2- to 3-cm-wide zone along the boundary of the box. However, my observations were made along vertical cross sections, which were cut in the middle of the models (40 cm wide), after 8.5, 20.4 and 23.8 % bulk shortening (see Eq. 1 in “Appendix”) for each model, away from the boundary effect. Avoiding boundary effect in analogue models (Mukherjee et al. 2012) is a standard process in laboratory-based structural geological studies.

The models were shortened from one side at an average rate of 20 mm h<sup>-1</sup> (simulating 6–10 mm year<sup>-1</sup> in nature) to a total bulk shortening of 23.8 %. The moving wall extended down to the “basement” and shortened the basal PDMS layer as well as the whole package of the sand and glass beads resting above it.

In model 1, which simulated the northern part of Lurestan region, one-cm-thick viscous layer of PDMS, simulating Hormuz salt (or Paleozoic shale), was acting as a viscous basal decollement the model (Fig. 3). The PDMS layer was then covered with layers of loose sand and glass beads. A 2-cm-thick layer of glass beads simulated a thick intermediate decollement in northern part of the Lurestan region (Fig. 3).

In model 2 (simulating the southern part of the Lurestan region), a similar 1-cm-thick viscous layer of PDMS was placed at the base of the model resting on the flat metal sheet. A 0.5-cm-thick layer of glass beads simulated a thinner intermediate decollement (Fig. 3).

The models are scaled with a geometric similarity (length ratio) of approximately 10<sup>-5</sup> such that 1 cm in the models simulates 1 km in nature. For dynamic similarity between a model and its natural prototype, a set of dimensionless ratios, which related to physical properties of the model materials and rocks, should be similar (Koyi and Petersen 1993; Weijermars et al. 1993; Nilforoushan et al. 2008). To achieve dynamic similarity in model and nature, the intrinsic material properties, such as cohesion ( $\tau_c$ ) and coefficient of internal friction ( $\mu$ ), need to be equal (Koyi and Petersen 1993; Weijermars et al. 1993). The internal friction angle of the upper crust rocks (<10 km) is averaged to 40° (Brace and Kohlstedt 1980), which gives a coefficient of internal friction of 0.84. The internal friction angle of uncompact loose sand used in the models is 36°, giving a coefficient of internal friction of 0.73. Cohesion, however, is scaled by equality between the non-dimensional shear strength both in the model and in nature:

$$(\rho l g / \tau_o)_m = (\rho l g / \tau_o)_n \quad (1)$$

where  $\rho$  is density,  $l$  is length,  $g$  is acceleration due to gravity, and the subscripts m and n denote the model and nature, respectively (Koyi and Petersen 1993; Weijermars et al. 1993; Nilforoushan et al. 2008). This non-dimensional ratio was calculated for the 1-g models and nature using the shear strength of sedimentary rocks to range between 1 and 10 MPa (Hoshino et al. 1972). For clastic sediments, the shear strength and the density have been taken 5 MPa and 2550 kg m<sup>-3</sup>, respectively. The loose sand acquired cohesion during scraping (collecting extra unwanted sand from the top surface of the sand layers in order to thickness adjustment). Its cohesion is ca. 140 Pa, and its density is 1550 kg m<sup>-3</sup>. These figures give the non-dimensional shear strength in Eq. (1) a value of  $1.6 \times 10^{-1}$  and  $7.5 \times 10^{-1}$  for model and nature, respectively. These two ratios, which are within the same order of magnitude, suggest that my 1-g models fulfill the criterion for dynamic similarity. For the ductile layer, dynamic similarity was achieved by simulating the ductile behavior of rock salt (or over pressured shale) with the Newtonian viscous material PDMS giving a viscosity scaling ratio of  $2.9 \times 10^{-14}$  to  $(-15)$ . Very high viscosity of rocks in collisional orogens (Mukherjee 2013b) is not attempted to match with the model material in analogue models.

## Model kinematics and results

During shortening, all materials resting on the flat metal sheet were deformed. Below, deformation of the two models (the “northern part of the Lurestan” and “southern part of the Lurestan”) is described in section view at three different stages of bulk shortening (8.5, 20.4 and 23.8 %).

### *Model 1: viscous (PDMS) basement with thick intermediate decollement layer simulating the northern part of the Lurestan (Fig. 4)*

The compressional structures (fore thrusts and fault-related asymmetric folds) formed in the model where the 20-mm-thick intermediate decollement exists within the cover layers after 8.5 % of shortening. Detached small folds were formed in deformation front above the 20-mm-thick intermediate decollement where deformation had propagated faster comparing to the layers beneath the intermediate decollement. The width of the deformation zone in this section (WDZ, the distance between the moving wall and the deformation front) within the layers above the intermediate decollement is further (ca. 9 cm) compared to the layers beneath it, after 8.5 % of bulk shortening (Fig. 4). This difference in propagation between the layers above and beneath the intermediate decollement is manifested in disharmonic deformation of the section from surface to deeper parts. This disharmony between the layers above and beneath the intermediate decollement

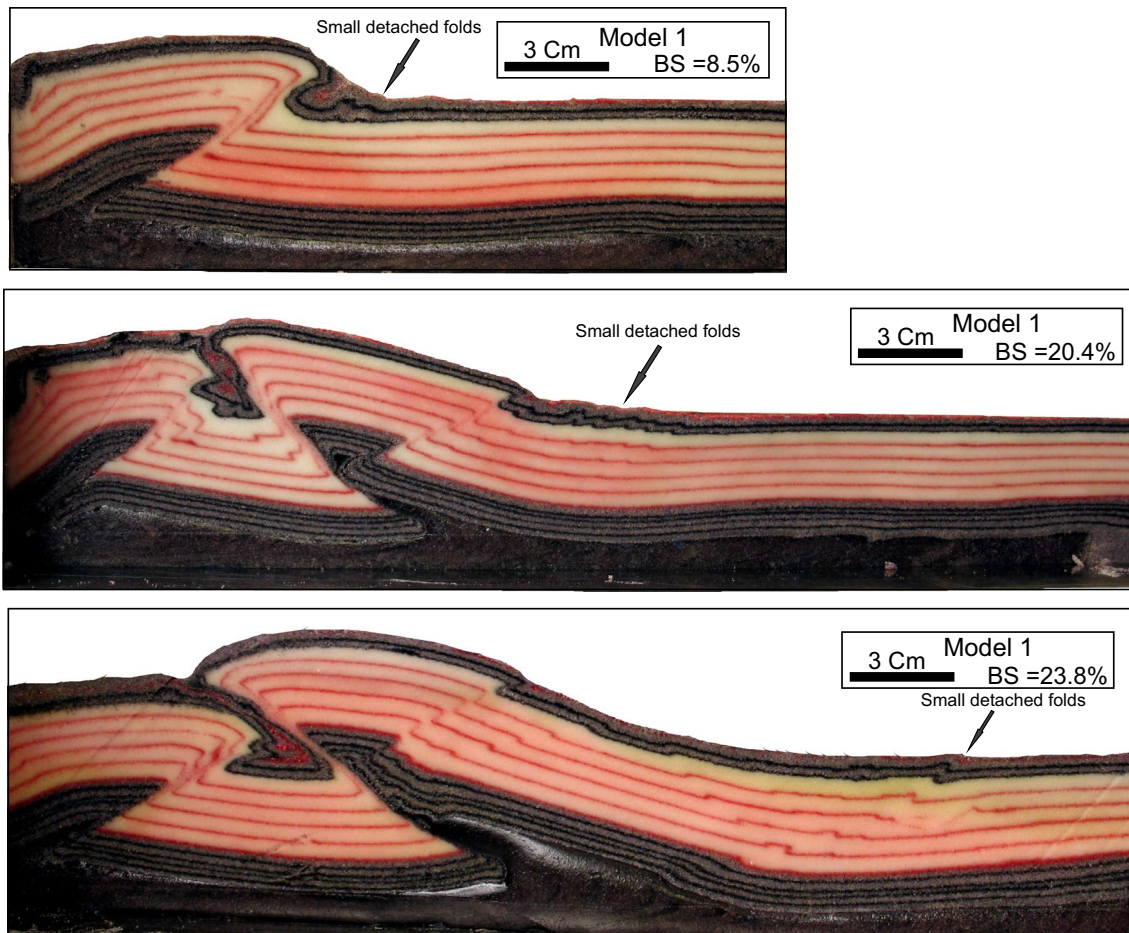


**Fig. 4** Section view photographs from different stages of shortening for model 1. Disharmony between the layers above and beneath the intermediate decollement is accommodated by activation of 20-mm-

thick glass beads layer as a weak horizon within the relatively more competent layers of loose sand (see "Discussion")

is accommodated by the activation of 20-mm-thick glass beads layer as a weak horizon within the relatively more competent layers of loose sand. After 20.4 % of bulk shortening, the WDZ in the section was 192 mm, and fore-and-back thrusts and fault-related folds were formed. Backthrusting is common in collisional orogens (Mukherjee 2013a). No out-of-sequence thrusts (Mukherjee 2015) were produced in the present models. Several small folds detached above the intermediate decollements were visible in sections (Fig. 4).

The WDZ reached 259 mm after 23.8 % of bulk shortening (Fig. 4). Although the main larger-scale fore-and-back thrusts and their related folds seemed to be clearer at this stage, several detached thrusts above the intermediate decollement were still visible and demonstrated disharmonic deformation within the layers above and beneath the intermediate decollement. Also faster propagation of deformation within the layers above the intermediate decollement, compared with the layers beneath it, was clear.

*Model 2: viscous (PDMS) basement with thin intermediate decollement layer simulating the southern part of the Lurestan (Fig. 5)*

In this model also, the first compressional structures (fore-and-back thrusts, pop-up and associated folds) appeared after 8.5 % bulk shortening. At this stage, there were no detached folds above the intermediate decollement. Shortening produced sharp pop-up structures and symmetric folds. The WDZ is 120 mm after 8.5 % of bulk shortening which is further compared to model 1 at this stage. After 20.4 % of shortening, lack of detached folds is very dominant compared to model 1 at the same amount of the bulk shortening (Figs. 4, 5). In profiles, harmonic geometry of deformation within the layers above and beneath the 5-mm-thick glass beads was visible.

The WDZ within the section reached 183 mm after 20.4 % and 229 after 23.8 % of bulk shortening (Fig. 5). These figures are less than those in model 1 with the same

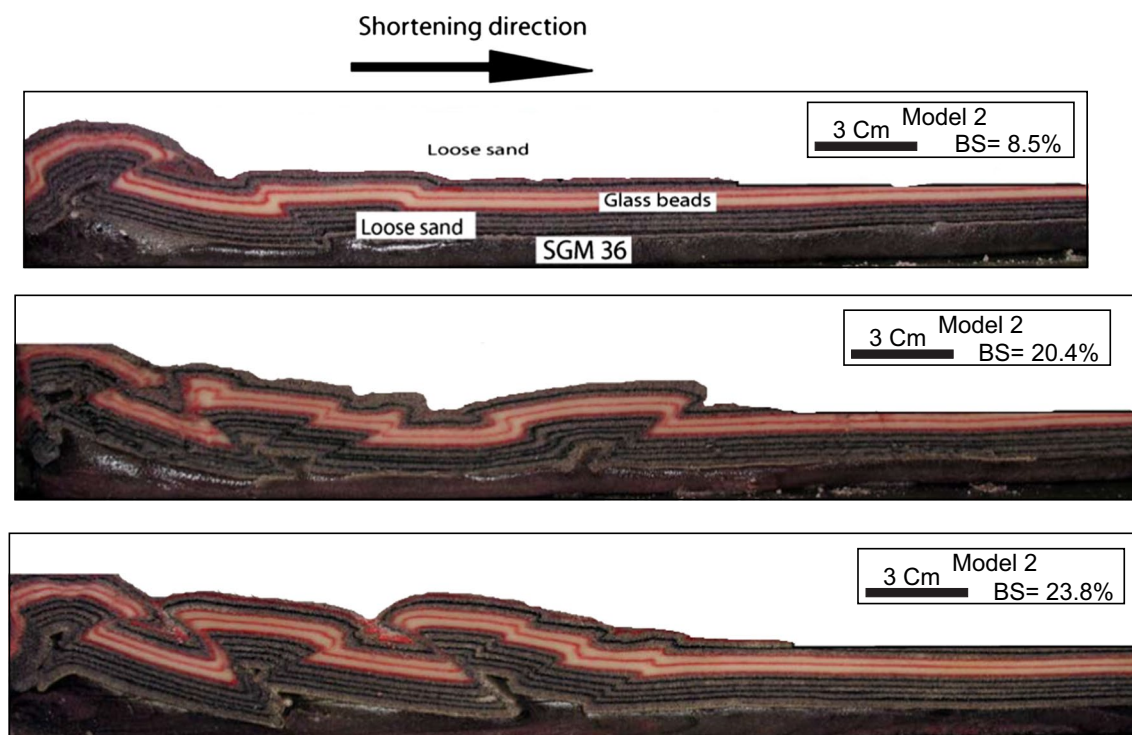


**Fig. 5** Section view photographs from different stages of shortening for model 2. Harmonic geometry of deformation within the layers above and beneath the 5-mm-thick glass beads is dominant compared to model 1 (see "Discussion")

amount of bulk shortening. Pop-up structures (related to fore-and-back thrusts), their relevant symmetric folds and lack of detached folds above the intermediate decollement were still visible at these stages also. In summary, following different stages of bulk shortening in this model demonstrated that by increasing the amount of shortening, deformation disharmony between the layers above and the layers beneath the intermediate decollement was very low compared to model 1. In other words, opposite to model 1, there is no complexity in surface folds relative to folding style at deeper parts of the section.

## Discussion

Several analogue modeling studies have focused on the effect of different rheological decollements (frictional and viscous) on deformation style in fold-and-thrust belts (e.g., Chapple 1978; Davis and Engelder 1985; Koyi 1988; Cobbold et al. 1989; Dixon and Liu 1992; Talbot 1992; Letouzey et al. 1995; Cotton and Koyi 2000; Koyi et al. 2000; Costa and Vendeville 2002; Bahroudi and Koyi 2003; Nilforoushan and Koyi 2007; Farzipour Saein and Koyi 2014). The effect of basal decollement on deformation and kinematics of fold-and-thrust belts has been discussed for different compressional belts; however, role of intermediate

decollement thickness change on folding style is less frequently discussed (see Harrison and Bally 1988; Koyi and Sans 2003; Bonini 2003; Koyi et al. 2004; Sherkati et al. 2005; Massoli et al. 2006; Farzipour Saein et al. 2009; Casciello et al. 2009; Vergés et al. 2011; Farzipour Saein and Koyi 2014). The relatively well-known stratigraphy and available surface structures in the northern and southern parts of the Lurestan region make the area an ideal place to apply model results to it. Natural weak basal or intermediate decollement horizons change gradually or abruptly to a frictional or less viscous decollement due to facies and/or simply thickness change, and such changes play a significant role in deformation style of an area (Cotton and Koyi 2000; Farzipour Saein et al. 2009; Farzipour Saein and Koyi 2014).

Our models, similar to other studies (e.g., Cotton and Koyi 2000; Farzipour Saein et al. 2009; Farzipour Saein and Koyi 2014), illustrate different deformation styles within the cover units as a result of lateral changes in detachment rheology. However, unlike Cotton and Koyi (2000) who focused only on lateral facies change of the basal decollement layer and Farzipour Saein and Koyi (2014) who demonstrated effect of lateral facies change in the intermediate decollement on the deformation front, this study looks into effect of different thicknesses of the intermediate decollement on folding style. The difference in deformation style

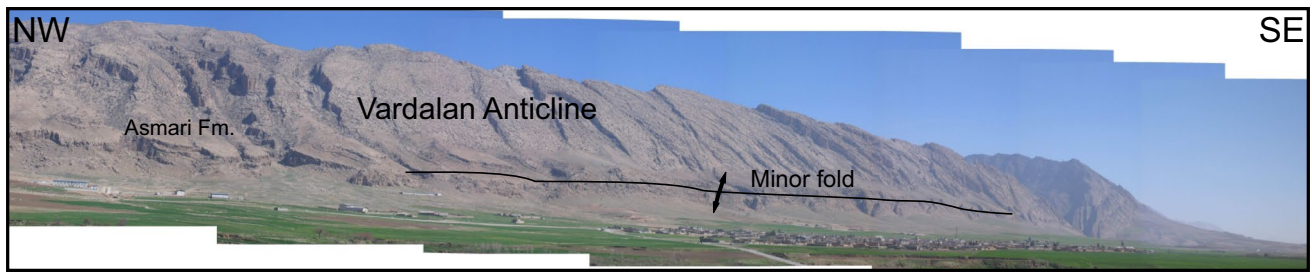


**Fig. 6** A minor detached folding in Asmari Fm. above the tectonically thickened intermediate decollements throughout the northern part of the study area, representing detached small folds above the

thick intermediate decollement (southern flank of the Vardalan anticline). See (Fig. 1), for the locations



**Fig. 7** Different deformation styles within an incompetent unit (Pabdeh Fm.) and competent unit (Asmari Fm.) at eastern plunch of the Sartang anticline, representing disharmonic folding at the northern part of the Lurestan. See (Fig. 1) for the locations

above frictional and viscous basal decollements has also been known and acknowledged before (e.g., Davis and Engelder 1985). Using geological and geophysical data, Farzipour Saein et al. (2009) and Vergés et al. (2011) studied the effect of lateral change in the intermediate decollement for northern and southern parts of the Lurestan region (Fig. 1). Folding style, laterally and vertically, showed two distinct patterns for the southern and northern parts of the Lurestan region (Farzipour Saein et al. 2009; Fig. 2).

In the models, since the same basal decollement but thickness of the intermediate decollement was varied, several minor detached folds formed above the thicker

intermediate decollement (model 1, Figs. 2, 4). Model 1 can be compared with the northern part of the Lurestan region, where a thick intermediate decollement is present within the sedimentary cover (Figs. 1, 2). In this part of the area, however, the more pelagic, more incompetent facies of the Sarvak and Pabdeh–Gurpi Formations (Farzipour Saein et al. 2009), as well as the thicker intermediate decollement level, causes decoupling of the overlying anticlines (Fig. 1). Consequently, the Paleozoic competent unit does not control the folding geometry of the whole sedimentary package and the folding style within the Paleozoic units is completely different from that observed in the sedimentary

layers above the intermediate decollement level (Fig. 2). In addition, the small-wavelength folds in the Asmari Formation (Figs. 2, 6), lying above the tectonically thickened intermediate decollement level, are decoupled from the deeper folds (Figs. 1, 4, 7). Thus, in the northern part of the Lurestan region, folding pattern is strongly disharmonic and the fold geometry at different structural levels (across the various decollement levels) is variable (Figs. 1, 4, 7). This folding style is comparable with the fold appeared above the intermediate decollement in model 1 where there is a thick intermediate decollement. The high thickness of the intermediate decollement (in model 1) permits more dominant activity of the intermediate decollement and increases its role in folding evolution of the whole sedimentary package (Fig. 4). This model shows several detached folds above the intermediate decollement. Increasing the amount of the bulk shortening for the models causes more detached folds above the intermediate decollement and consequently disharmonic folding within the section. In early stages of model deformation, a gentle large-scale fold is created. Due to the presence of a thick intermediate decollement, shortening was accommodated by the intermediate decollement and the layers located above it detaching them from the lower units. Thus, this intermediate decollement causes disharmonic folding. This also leads to faster propagation of deformation within the sediments above the intermediate decollement and causes disharmonic folding, following folding geometry from surface to deeper parts of the section (Fig. 4).

Model 2 can be compared with the southern part of the Lurestan, where a thinner intermediate decollement (compared to the northern part and model 1) is present within the cover unit (Figs. 1, 2). The effective and major role of the basal decollement on deformation in this model (similar to model 1) causes the whole pile of sand bed detached from the metal sheet (the basement). With further bulk shortening, the viscous PDMS migrates gradually from synclines to the core of the adjacent anticlines. Consequently, the model shows nucleation of the fore-and-back thrusts and their relevant folds (Fig. 5). During this process, there is no activation of the intermediate decollement in order to accommodate the deformation, compared to model 1 (Figs. 4, 5). This scenario could simulate the southern part of the Lurestan, where the main role of the basement decollement (thick Hormuz salt or Paleozoic sediments) on evolution of the anticlines has been documented (Farzipour Saein et al. 2009). In the southern part of the region, the intermediate decollement level is thinner and more competent units exist within the stratigraphic column (Paleozoic competent units, the Ilam limestone and shallow marine, neritic facies of the Sarvak Formations; Farzipour Saein et al. 2009; Figs. 1, 2). Consequently, the folds in the Sarvak Formation show larger wavelengths, which govern the geometry of the layers above them (Fig. 2). In spite of the

small folds within the Cretaceous and Jurassic formations, which reflect the minor effect of the Triassic intermediate decollement level, the thick Paleozoic competent unit controls the general fold geometry of the whole package (polyharmonic folding) (Koyi 1988; Farzipour Saein et al. 2009; Fig. 2). This is because of the more competent neritic portion of the Sarvak Formation (Farzipour Saein et al. 2009) which causes preservation of the longer wavelength folds all the way to the surface (i.e., coupling between deep and shallow structures; Figs. 2, 5). Indeed, polyharmonic folding style (Farzipour Saein et al. 2009), model 2 with thinner intermediate decollement, could be concluded as the major and stronger activity of the basal decollement as main controller of folding style within the whole pile of the sediments (Figs. 2, 5).

In general, the models showed that presence of the thick intermediate decollement (simulating the northern part of the Lurestan) can give rise to faster propagation of the deformation front and larger WDZ, in comparison with the model having the thinner intermediate decollement (simulating the southern part of the Lurestan) (Farzipour Saein and Koyi 2014). However, faster deformation propagation of the sediments above the intermediate decollement compared with the sediments beneath it is obvious for both models.

Finally, model 1 confirms that intermediate decollement horizon decouples shallow and deeper units; i.e., subsurface structures and their characteristics cannot always dictate the location of the surface structures exactly above them. It may lead to draw wrong conceptual tectonic profile from the structural data collected at the surface exposure. I do believe that such decoupling occurs between deep and shallow structures in different parts of the Zagros, where there are intermediate decollement units with sufficient thickness.

## Conclusions

Results of scaled models were combined with geological observation to argue the lateral facies change of sedimentary rocks and consequently thickness change of the intermediate decollement within the Zagros stratigraphy. Thickness change of the intermediate decollement resulted in different folding style at the northern and southern parts of the Lurestan region. These findings can be applied to other areas where intermediate weak (incompetent) horizons are present within the shortened stratigraphy.

The model that was shortened above the viscous decollement, however, with the thicker intermediate decollement propagated further and faster than the other that were shortened with the thinner intermediate decollement, and it showed the largest WDZ at the final stage of the shortening. In other words, the basal decollement characteristics

have dominant and major role in controlling the deformation style, where the intermediate decollement has no sufficient thickness.

The presence of a thick intermediate decollement can give rise to faster propagation of the deformation in the sediments above it compared to the sediments beneath it especially where it is thick enough to be active as a main decollement within the sedimentary pile during compression. This will form detached minor folds above the intermediate decollement (or above a single larger anticline beneath it). Thus, the deformation complexity and disharmonic folding style exist in the section that the intermediate decollement has been activated in response to the shortening. In other words, the deformation complexity of the section (with the same basal decollement) is getting minor when the thickness of the intermediate decollement in the model decreases. Model 1 and model 2 simulate their prototype (the northern and southern parts of the Lurestan region), respectively.

Finally, the model results could help to establish that, in addition to other parameters, not presented in this study, thickness variation of intermediate decollement levels could explain complex and different folding styles in natural examples which must be taken into account for hydrocarbon exploration throughout these areas with varied intermediated decollement units within its sedimentary pile, e.g., the Lurestan region.

**Acknowledgments** The research and postgraduate office at University of Isfahan is thanked for their support. I also acknowledge Prof. Hemin Koyi for giving me the opportunity to run the models at Hans Ramberg Tectonic Laboratory. Soumyajit Mukherjee handled this manuscript and provided a review. Review by another person is also thanked.

## Appendix

Bulk shortening for each stage was calculated by taking the length difference between the moving wall and back wall of the model at each stage, to the original difference between them (before shortening) using:

$$e = L - L_0/L_0 \times 100.$$

Equation 1: percent shortening calculation ( $e$ ) where  $L$  is the length measured and  $L_0$  is the original length.

## References

Ahmadhadi F, Lacombe O, Daniel J-M, (2007) Early reactivation of basement faults in Central Zagros (SW Iran): evidence from pre-folding fracture populations in Asmari formation and lower

- tertiary paleogeography. In: Lacombe O (ed) Thrust belts and foreland basins: from fold kinematics to hydrocarbon systems. Springer, p 224. ISBN 978-3-540-69425-0
- Bahroudi A, Koyi HA (2003) The effect of spatial distribution of Hormuz salt on deformation style in the Zagros fold and thrust belt: an analogue modeling approach. *J Geol Soc (Lond)* 160:719–733
- Bahroudi A, Koyi HA (2004) Tectono-sedimentary framework of the Gachsaran formation in the Zagros foreland basin. *Mar Petrol Geol* 21:1295–1310
- Berberian M (1995) Master blind thrust faults hidden under the Zagros folds: active basement tectonics and surface morphotectonics. *Tectonophysics* 241:193–224
- Berberian M, King GCP (1981) Towards the paleogeography and tectonic evolution of Iran. *Can J Earth Sci* 18:210–265
- Blanc EJ-P, Allen MB, Inger S, Hassani H (2003) Structural style in the Zagros simple folded zone, Iran. *J Geol Soc Lond* 160:401–412
- Bonini M (2001) Passive roof thrusting and foreland ward fold propagation in scaled brittle-ductile physical models of thrust wedges. *J Geophys Res* 106(B2):2291–2311
- Bonini M (2003) Detachment folding, fold amplification, and diapirism in thrust wedge experiments. *Tectonics* 22(6):1065. doi:10.1029/2002TC001458
- Brace WF, Kohlstedt D (1980) Limits on lithospheric stress imposed by laboratory measurements. *J Geophys Res* 85:6248–6252
- Buchanan PG, McClay KR (1991) Sandbox experiments of inverted listric and planar fault systems. *Tectonophysics* 188:97–115
- Butler RWH, Coward MP, Harwood GM, Knipe R (1987) Salt: its control on thrust geometry, structural style and gravitational collapse along the Himalayan Mountain front in the Salt Range of northern Pakistan. In: Lerche I, O'Brien JJ (eds) *Dynamical geology of salt and related structures*. Academic Press, Orlando, pp 339–418
- Casciello E, Vergés J, Saura E, Casini G, Fernández N, Blanc E, Homke S, Hunt DW (2009) Fold patterns and multilayer rheology of the Lurestan Province, Zagros Simply Folded Belt (Iran). *J Geol Soc* 166:947–959
- Chapple WM (1978) Mechanics of a thin-skinned fold-and-thrust belt. *Geol Soc Am Bull* 89:1189–1198
- Cobbold PR, Rossello EA, Vendeville B (1989) Some experiments on interacting sedimentation and deformation above salt horizons. *Bulleten de la Societe Geologique de France* 8:453–460
- Cobbold PR, Szatmari P, Demercian LS, Coelho D, Rossello EA (1995) Seismic and experimental evidence for thin-skinned horizontal shortening by convergent radial gliding on evaporites, deep-water Santos Basin, Brazil. In: Jackson MPA, Roberts DG, Snelson S (eds) *Salt tectonics: a global perspective*, vol 65. American Association of Petroleum Geologists Memoir, pp 305–321
- Costa E, Vendeville BC (2002) Experimental insights on the geometry and kinematics of fold-and-thrust belt above weak, viscous evaporitic decollement. *J Struct Geol* 24:1729–1739
- Cotton JT, Koyi HA (2000) Modeling of thrust fronts above ductile and frictional detachments: application to structures in the Salt Range and Potwar Plateau, Pakistan. *Geol Soc Am Bull* 112:351–363
- Davis DM, Engelder T (1985) The role of salt in fold-and-thrust belts. *Tectonophysics* 119:67–88
- Davy P, Cobbold PR (1991) Experiments on shortening of 4-layer model of continental lithosphere. *Tectonophysics* 188:1–25
- Dixon JM, Liu S (1992) Centrifuge modeling of the propagation of thrust faults. In: McClay KR (ed) *Thrust tectonics*. Chapman and Hall, London, pp 53–69
- Falcon N (1969) Problems of relationship between surface structure and deep displacement illustrated by Zagros. In: Kent PE, Satterthawate GE, Spencer AM (eds) *Time and place in Orogeny*, vol 2. Geological Society of London, Special Publication, pp 9–22

- Falcon NL (1974) Southern Iran: Zagros Mountains. In: Spencer A (ed) Mesozoic-Cenozoic Orogenic belts, vol 4. Geological Society of London, Special Publication, pp 199–211
- Farzipour Saein A, Koyi H (2014) Effect of lateral thickness variation of an intermediate decollement on the propagation of deformation front in the Lurestan and Izeh zones of the Zagros fold-thrust belt, insights from analogue modeling. *J Struct Geol* 65:17–32
- Farzipour Saein A, Yassagi A, Sherkati S, Koyi H (2009) Mechanical stratigraphy and folding style of the Lurestan region in the Zagros Fold Thrust Belt, Iran. *J Geol Soc* 166:1101–1115
- Farzipour Saein A, Nilforoushan F, Koyi H (2013) The effect of basement step/topography on the geometry of the Zagros fold and thrust belt (SW Iran): an analogue modeling approach. *Int J Earth Sci*. doi:10.1007/s00531-013-0921-5
- Harrison JC, Bally AW (1988) Cross sections of the Devonian to Mississippian fold belt on Melville Island, Canadian arctic islands: implication for the timing and kinematic history of some thin-skinned decollement systems. *Bull Can Pet Geol* 36:311–332
- Harrison HL, Pattern BD (1995) Translation of salt sheets by basal shear. In: Salt sediments and hydrocarbons, Gulf Coast Section SEPM Foundation 16th Annual Conference, December 3–6, 99–107
- Haynes SJ, Mcquillan H (1974) Evolution of the Zagros suture zone, southern Iran. *Geol Soc Am Bull* 85:739–744
- Hessami K, Koyi HA, Talbot CJ, Tabasi H, Shabanian E (2001a) Progressive unconformities within an evolving foreland fold-thrust belt, Zagros Mountains. *J Geol Soc Lond* 158:969–981
- Hessami K, Koyi HA, Talbot CJ (2001b) The significance of strike-slip faulting in the basement of the Zagros fold-thrust belt. *J Pet Geol* 24:5–28
- Homke S, Vergés J, Garcés M, Emami H, Karpuz R (2004) Magnetostratigraphy of Miocene–Pliocene Zagros foreland deposits in the front of the Push-e Kuh Arc (Lurestan province, Iran). *Earth Planet Sci Lett* 225:397–410
- Hoshino K, Koide H, Inami K, Iwamura S, Mitsui S (1972) Mechanical properties of Japanese tertiary sedimentary rocks under high confined pressure. *Geol Surv Jpn Rep* 244:1–200
- Koyi HA (1988) Experimental modeling of the role of gravity and lateral shortening in the Zagros mountain belt. *Am Assoc Pet Geol Bull* 72:381–1394
- Koyi H, Petersen K (1993) The influence of basement faults on the development of salt structures in the Danish Basin. *Marin Petrol Geol* 10:82–94
- Koyi HA, Sans M (2003) Modelling the effect of multiple detachments in fold-thrust belts. AAPG International Meeting, Barcelona, p A51
- Koyi HA, Hessami K, Teixell A (2000) Epicenter distribution and magnitude of earthquakes in fold-thrust belts: insights from sandbox models. *Geophys Res Lett* 27:273–276
- Koyi HA, Sans M, Bahroudi A (2004) Modeling the deformation front of fold-thrust belts containing multiple weak horizons. *Bollettino di Geofisica Teorica Application* 45:101–103
- Letouzey J, Colletta B, Villay R, Chermette JC (1995) Evolution of salt related structures in compressional setting. In: Jackson MPA, Roberts DG, Snelson S (eds) Salt tectonic: a global perspective, vol 65. American Association of Petroleum Geologists Bulletin Memoir, pp 41–60
- Liu H, McClay KR, Powell D (1992) Physical models of thrust wedges. In: McClay KR (ed) Thrust tectonics. Chapman and Hall, London, pp 71–81
- Massoli D, Koyi HA, Barchi MR (2006) Structural evolution of a fold and thrust belt generated by multiple decollements: analogue models and natural examples from the Northern Apennines (Italy). *J Struct Geol* 28:185–199. doi:10.1016/j.jsg.2005.11.002
- McClay KR (1989) Analogue models of inversion tectonics. In: Cooper MA, Williams GD (eds) Inversion tectonics, vol 44. Geological Society [London] Special Publication, pp 41–59
- Mcquillan H (1991) The role of basement tectonics in the control of sedimentary facies, structural patterns and salt plug emplacement in the Zagros fold belt of southwest Iran. *J Southeast Asian Earth Sci* 5(4):453–463
- Molinaro M, Leturmy P, Guezou JC, Frizon de Lamotte D, Eshraghi SA (2005) The structure and kinematics of the south-eastern Zagros fold-thrust belt, Iran: from thin skinned to thick skinned tectonics. *Tectonics*. doi:10.1029/2004Tc001633
- Motiee H (1994) Stratigraphy of Zagros. Geological Survey of Iran Publications, Tehran (in Farsi)
- Mukherjee S (2013a) Higher Himalaya in the Bhagirathi section (NW Himalaya, India): its structures, backthrusts and extrusion mechanism by both channel flow and critical taper mechanisms. *Int J Earth Sci* 102:1851–1870
- Mukherjee S (2013b) Channel flow extrusion model to constrain dynamic viscosity and Prandtl number of the Higher Himalayan Shear Zone. *Int J Earth Sci* 102:1811–1835
- Mukherjee S (2015) A review on out-of-sequence deformation in the Himalaya. In: Mukherjee S, Carosi R, van der Beek P, Mukherjee BK, Robinson D (eds) Tectonics of the Himalaya, vol 412. Geological Society, London. Special Publications, pp 67–109
- Mukherjee S, Biswas R (2015) Biviscous horizontal simple shear zones of concentric arcs (Taylor Couette flow) with incompressible Newtonian rheology. In: Mukherjee S, Mulchrone KF (eds) Ductile shear zones: from micro- to macro-scales. Wiley Blackwell, Chichester, pp 59–62
- Mukherjee S, Mulchrone KF (eds) (2015) Ductile shear zones: from micro- to macro-scales. Wiley Blackwell, Chichester
- Mukherjee S, Talbot C, Koyi HA (2010) Viscosity estimates of salt in the Hormuz and Namakdan salt diapirs, Persian Gulf. *Geol Mag* 147:497–507
- Mukherjee S, Koyi HA, Talbot CJ (2012) Implications of channel flow analogue models in extrusion of the higher Himalayan shear zone with special reference to the out-of-sequence thrusting. *Int J Earth Sci* 101:253–272
- Mulchrone KF, Mukherjee S (2015) Shear senses and viscous dissipation of layered ductile simple shear zones. *Pure Appl Geophys* 172:2635–2642
- Nilforoushan F, Koyi HA (2007) Displacement fields and finite strains in a sandbox model, simulating a fold-thrust belt. *Geophys J Int* 169:1341–1355. doi:10.1111/j.1365-246X.2007.03341.x
- Nilforoushan F, Koyi HA, Swantesson JOH, Talbot CJ (2008) Effect of basal friction on surface and volumetric strain in models of convergent settings measured by laser scanner. *J Struct Geol* 30:366–379
- O'Brien CAE (1950) Tectonic problems of the oilfield belt of southwest Iran. In: 18th International geological congress, proceedings, Great Britain
- O'Brien CAE (1957) Salt diapirism in south Persia. *Geol Mijnb* 19:357–376
- Price NJ, Cosgrove JW (1990) Analysis of geological structures, vol 502. Cambridge University Press, Cambridge
- Sans M, Vergés J (1995) Fold development related to contractional salt tectonics: southeastern Pyrenean thrust front, Spain. In: Jackson MPA, Roberts DG, Snelson S (eds) Salt tectonics: a global perspective, vol 65. American Association of Petroleum Geologists Memoir, pp 369–378
- Sepehr M, Cosgrove JW (2004) Structural framework of the Zagros Fold-Thrust Belt, Iran. *Mar Pet Geol* 21:829–843
- Sepehr M, Cosgrove JW, Moieni M (2006) The impact of cover rock rheology on the style of folding in the Zagros fold-thrust belt. *Tectonophysics* 427:265–281
- Sherkati S, Letouzey J (2004) Variation of structural style and basin evolution in the central Zagros (Izeh zone and Dezful embayment), Iran. *Mar Pet Geol* 21:535–554
- Sherkati S, Molinaro M, Frizon de Lamotte D, Letouzey J (2005) Detachment folding in the Central and Eastern Zagros fold-belt

- (Iran): salt mobility, multiple detachments and late basement control. *J Struct Geol* 27:1680–1696
- Sherkati S, Letouzey J, Frizon de Lamotte D (2006) Central Zagros fold- thrust belt (Iran): new insights from seismic data, field observation and sandbox modeling. *J Tectonics*. doi: [10.1029/2004TC001766](https://doi.org/10.1029/2004TC001766)
- Stocklin J (1968) Structural history and tectonics of Iran; a review. *Am Assoc Pet Geol Bull* 52:1229–1258
- Talbot CJ (1992) Centrifuge models of Gulf of Mexico profiles. *Mar Pet Geol* 9:412–432
- Treloar PJ, Coward MP, Chambers AF, Izatt CN, Jackson KC (1992) Thrust geometries and rotations in the northwest Himalaya. In: McClay KR (ed) *Thrust tectonics*. Chapman and Hall, London, pp 325–343
- Vergés J, Goodarzi MGH, Emami H, Karpuz R, Efstathiou J, Gillespie P (2011) Multiple detachment folding in Pusht-e Kuh arc, Zagros: role of mechanical stratigraphy. *AAPG Mem* 94 Chapter 4, 69–94
- Weijermars R (1986) Flow behavior and physical chemistry of bouncing putties and related polymers in view of tectonic laboratory applications. *Tectonophysics* 124:325–358
- Weijermars R, Jackson MPA, Vedeville BC (1993) Rheological and tectonic modeling of salt provinces. *Tectonophysics* 217:143–174
- Weimer P, Buffler RT (1992) Structural geology and evolution of the Mississippi fan foldbelt, deep Gulf of Mexico. *Am Assoc Pet Geol Bull* 76:225–251